ELSEVIER

Journal of Alloys and Compounds 452 (2008) 200–204

Journal of ALLOYS AND COMPOUNDS

www.elsevier.com/locate/jallcom

Electrical and thermoelectric properties of PbSe doped with Sm

M.M. Ibrahim, S.A. Saleh *, E.M.M. Ibrahim, A.M. Abdel Hakeem

Physics Department, Faculty of Science, Sohag University, Sohag, Egypt

Received 31 July 2006; received in revised form 5 November 2006; accepted 6 November 2006
Available online 14 December 2006

Abstract

The electrical conductivity (σ), Seebeck coefficient (S) and power factor ($S^2\sigma$) of $Pb_{1-x}Sm_xSe$ ($x = 0.00$, 0.03, 0.06 and 0.09) annealed at 215 °C for different time periods have been investigated in the temperature range of 90–450 K to explore the effect of Sm doping and time of annealing on the PbSe thermoelectric performance. The XRD analysis does not exhibit any deviation from the characterizing rock-salt structure with changing the Sm amount or annealing time. Increasing Sm content resulted in increasing the activation energy as the character of other magnetic dopants. The thermoelectric measurements show that all samples are n-type semiconductor and the modulus value of Seebeck coefficient increases with increasing Sm content from $x = 0.00$ to 0.06. The highest value of power factor 83.8 $\mu W\,cm^{-1}\,K^{-2}$ has been recorded for $Pb_{0.94}Sm_{0.06}Se$ sample annealed for 180 min. The results indicate that samarium can be introduced as a dopant for PbSe to enhance its thermoelectric performance.

Keywords: PbSe; Annealing; Thermoelectric materials; Power factor

1. Introduction

Lead chalcogenides have been involved in many applications. They have been used as sensors for infrared radiation, photoresistor, lasers, solar cells, optoelectronic devices and thermoelectric devices [1–9]. Thermoelectric devices have been used practically in wider areas recently, such as in consumer products like small refrigerators and in high-tech applications like in cooling units for fiber junctions in optical fiber communication technology [10,11]. They are reliable energy converters and have no noise or vibration, as there are no mechanical moving parts [12,13]. Also devices based on this technology can be manufactured at very small size, which enables application to very local area with precise temperature control [10–13].

There were interests to introduce PbSe compounds by many researchers as thermoelectric materials for cooling and power generation applications. The power factor (Pf) is a good monitor for the thermoelectric (TE) performance. Since it is given as $Pf = S^2\sigma$, where S is the Seebeck coefficient and σ is the electrical conductivity, it is carrier concentration dependant. Story [14] reported that IV–VI compounds allow for simple control of carrier concentration by means of doping and isothermal annealing. So, TE performance could be enhanced by optimizing both the doping and thermal treatment processes.

The effect of thermal treatment had been tested by many researchers [15–20]. For instance, Unuma et al. [18] measured the Seebeck coefficient and electrical conductivity in a temperature range from room temperature to 600 K in argon atmosphere for pressureless-sintered PbSe ceramics. The results implied changing in temperature dependence of thermoelectric power and electrical conductivity by changing the sintering conditions. They reported that, increasing the sintering temperature is associated with changing the Seebeck coefficient sign and reducing the conductivity by one or two orders of magnitude.

Many researchers reported that, doping IV–VI semiconductors with variable values of elements results in appearance of a range of unusual effects that are not characterizing the undoped material, [14,21,22]. In the past, only the group III elements (AL, Ga, In, and Tl) represented the impurities of IV–VI compounds. However in recent publications the impurities elements were expanded to include Cr, Yb, Eu, Gd, and Ce transition elements. Doping with these elements transforms IV–VI semiconductors into semimagnetic semiconductors [21–28]. In the other side, Skipetrov et al. [29] reported that ytterbium doping modifies the energy spectrum of charge carriers in lead telluride by formation of deep impurity level. At low Ytterbium content this deep level is resonant with the valence band, however by increasing the impurity concentration it approaches the valence

* Corresponding author. Tel.: +20 104311140; fax: +20 934601159.
E-mail address: saleh2010_ahmed@yahoo.com (S.A. Saleh).

0925-8388/$ – see front matter © 2006 Published by Elsevier B.V.
doi:10.1016/j.jallcom.2006.11.049

band edge and shifts into the forbidden band. Also, the physical property of $Pb_{1-x}Eu_xSe$ is the rapid increase in the energy gap with increasing Eu content [10,30–32]. Another evidence for the influence of the doping process on the thermoelectric properties of IV–VI compounds was introduced by Su et al. [33]. They announced that for n-type lead telluride (PbTe) compounds doped with Sb_2Te_3, the electrical conductivity and the absolute value of Seebeck coefficient increase with increasing the Sb_2Te_3 content. The thermoelectric performance enhancement of PbTe in their study may be due to the high pressure under which the samples were prepared in addition to the low lattice thermal conductivity resulted from using Sb_2Te_3 as source of doping.

This work as a part of research plan [22] aims to introduce samarium as a dopant for PbSe compound and to optimize the doping level and thermal treatment conditions to obtain the best performance of $Pb_{1-x}Sm_xSe$ ($0 \le x \le 0.09$) as a thermoelectric material.

2. Experimental

The samples were prepared from high-purity (99.999%) elements obtained from Aldrich. The alloys were formed by direct melting the mixtures of the pure elements at 1100 °C in silica tube sealed under vacuum (10^{-5} Torr). The melting duration was 12 h with frequently agitation to ensure complete homogeneous mixing and it was followed with quenching in ice cold water. Then the quartz tube was broken and the ingots of the samples were grounded thoroughly for 2 h to obtain fine particles. This was ensured by sieving the powder by a sieve with apertures diameter equal to 63 μm. The powder of each composition was divided into equal amounts and pressed under 5 t/cm^2 to be in pellet form. The annealing process was performed at 215 °C for different time intervals 160, 180, 200, 220 and 240 min in vacuum controlled furnace. This temperature was chosen below the lowest invariant temperature of the constituent binary diagram of PbSe. The internal microstructure of the $Pb_{1-x}Sm_xSe$ ($x = 0$, 0.03, 0.06 and 0.09) system was characterized by X-ray diffraction (XRD) (Bucker Axs-D8 Advance diffractometer with Cu K_α radiation). The electrical and thermoelectric measurements have been carried out using especially made sample holder. Both of measurement processes were performed over temperature range 90–450 K in a vacuum 10^{-3} mmHg which was found to contribute much to the thermal stability during measurements. For the electrical measurements, a dry cell has been used as voltage source and the current was measured using Keithley's electrometer. The voltage in both types of measurements was measured using Keithley 182 sensitive digital voltmeter. The temperature of the specimen and temperature gradient in the thermoelectric measurement were sensed by standard copper-constantant thermocouples.

3. Results and discussion

The results of X-ray diffraction patterns are shown in Fig. 1. The d values are in good agreement with JCPDS data (see cart no. 6-354) confirming the rock salt (NaCl) structure of all the investigated samples [34–36]. In addition, the diffraction peaks corresponding to the ternary compounds of Pb_xSm_ySe are not found. This is expectable, because with Sm doping Pb^{2+} ions are substituted by Sm^{3+} ions [37] and the resultant SmSe system crystallizes also in NaCl structure [37,38]. The absence of the diffraction peaks corresponding to the ternary compounds matches well with Su et al. [33] whom pronounced that the ternary compounds of doped IV–VI compounds should not be formed with high cooling rate, small synthetic pressures and small dopant amounts which are the conditions of sample preparation in this work. Based on these results, the investigated samples are single phase PbSe while samarium is the source of dopant for PbSe. The presence of sharp structural peaks in the diffractograms suggests polycrystalline nature of the samples [36]. The appearance of the most prominent diffraction peak at 2θ equal to 29.2° which corresponds to (2 0 0) plane indicating the predominant growth of crystallites in this direction [36].

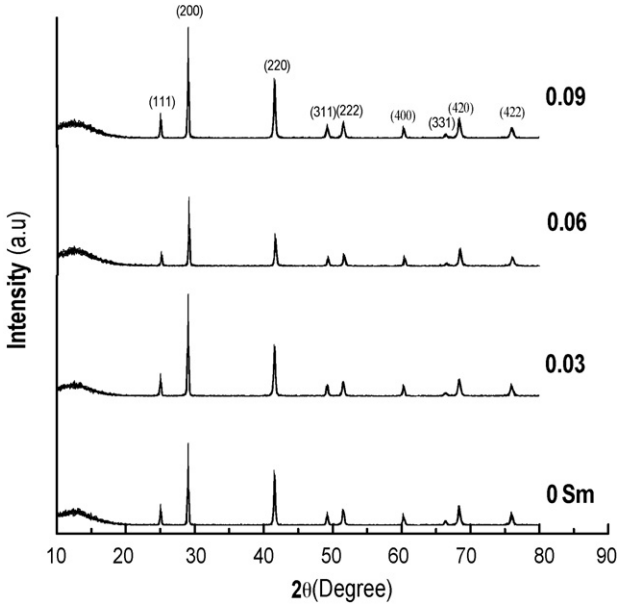

Fig. 1. XRD patterns of the alloys $Pb_{1-x}Sm_xSe$: (a) $x = 0.00$; (b) $x = 0.03$; (c) $x = 0.06$ and (d) $x = 0.09$.

Electrical conductivity is a prominent factor which reveals reliable information about the transport phenomena. As it was mentioned above, the temperature dependence of electrical conductivity for the samples of $Pb_{1-x}Sm_xSe$ ($x = 0.00$, 0.03, 0.06 and 0.09) compositions annealed at 215 °C for 160, 180, 200, 220 and 240 min has been tested in the temperature range $90 \le T \le 450$ K. In Fig. 2 the temperature variations of the electrical conductivity exhibit the characteristic extrinsic behavior of PbSe compositions [39,40] where the conductivity decreases with increasing temperature, reaches its minimum value at certain temperature T_s and then increases. At low temperature ($T < T_s$), the electrical conductivity is a characteristic of extrinsic conduction, while at higher temperature ($T > T_s$) the number of carriers thermally excited across the semiconducting energy gap begins to overwhelm the number of carriers due to ionized impurities and the intrinsic conduction begins to predominate [41,42]. In the intrinsic semiconductor behavior region, the temperature dependence of electrical conductivity can be fitted to the relation:

$$\sigma = \sigma_0 \exp\left(\frac{-E_\sigma}{k_B T}\right)$$

where σ_0 is the pre-experimental factor representing the temperature independent conductivity, and E_σ is the activation energy for conduction. The $\ln \sigma$ versus $1000/T$ plots in Fig. 3 are linear for all samples which confirm that the conduction in the concerned range of temperature is through thermally activated

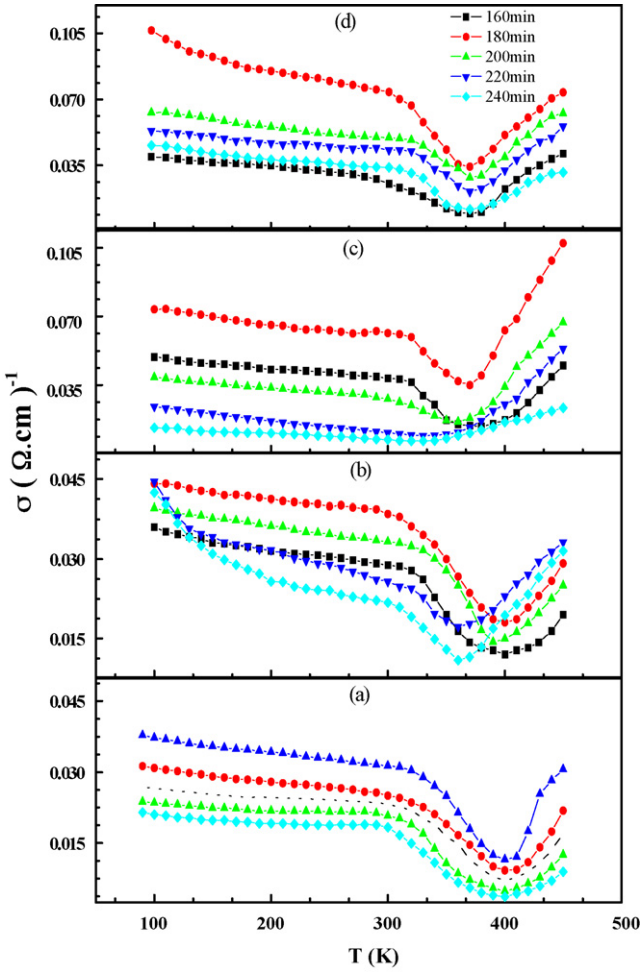

Fig. 2. Temperature dependence of electrical conductivity of the alloys $Pb_{1-x}Sm_xSe$: (a) $x=0.00$; (b) $x=0.03$; (c) $x=0.06$ and (d) $x=0.09$ annealed for different time periods.

process and the conductivity increasing with temperature is exponential. The thermally activated conduction in polycrystalline samples of lead chalcogenides has been proved by many researchers [36,43,44]. Fig. 4 shows the activation energy as a function of annealing time period for all compositions. It is clear that the activation energy for a certain composition decreases with elevating the annealing time from 160 to 240 min. However, its increase with increasing the magnetic ions (Sm) content is due to the impurity level movement into the forbidden gap [29,30–32].

In Fig. 5 the variation of Seebeck coefficient with $1000/T$ seem has similar behavior for all the considered samples no matter what the annealing time is. The sign of S is negative indicating typical n-type semiconductors for all annealing times and within the whole considered range of temperature. The absolute value of Seebeck coefficient S increases with increasing the ambient temperature T_{amb} in the low temperature range to its maximum at a certain temperature T_m and then decreases due to thermally excited carriers [41,45]. The effect of the grain boundary on the thermopower is much less than that on conductivity [46,47]. This induces the relatively lower values of T_m than T_s. Fig. 6 illustrates the dependence of the modulus

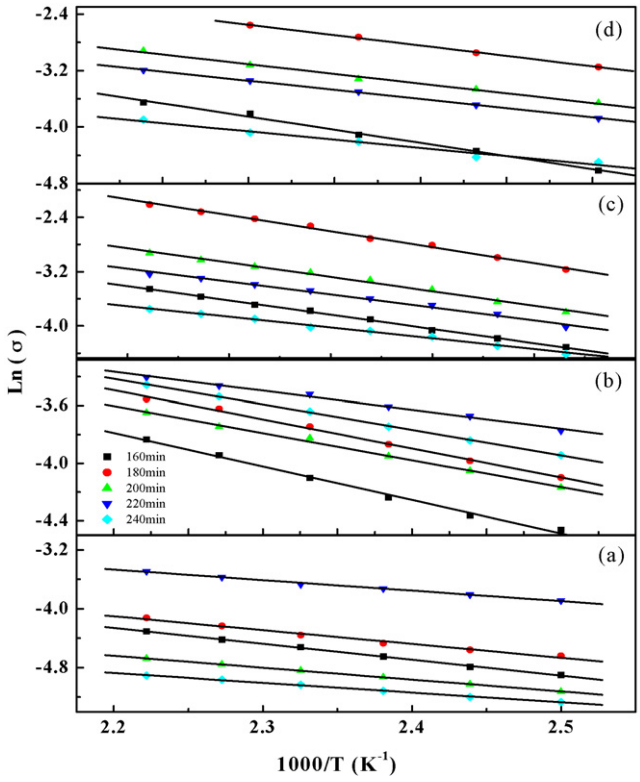

Fig. 3. $\ln(\sigma)$ vs. $1000/T$ plots of the alloys $Pb_{1-x}Sm_xSe$: (a) $x=0.00$; (b) $x=0.03$; (c) $x=0.06$ and (d) $x=0.09$ annealed for different time periods.

value of Seebeck coefficient S, at ambient temperature 250 K, on the Sm content. The results extracted that, the absolute value of S of PbSe samples are varying between 0.2 and 0.257 mV/K which is around previous published data [18,48]. The general

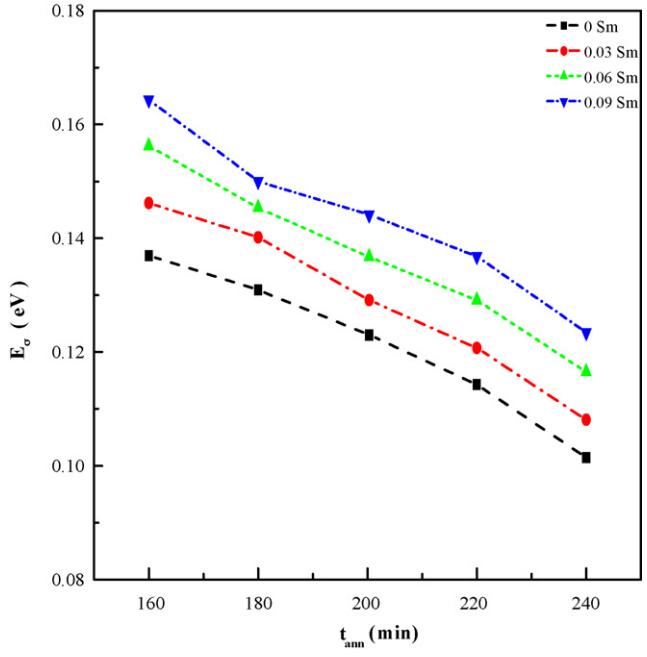

Fig. 4. Variation of the activation energy (E_σ) with annealing time (t_{ann}) of the alloys $Pb_{1-x}Sm_xSe$: (a) $x=0.00$; (b) $x=0.03$; (c) $x=0.06$ and (d) $x=0.09$ annealed for different time periods.

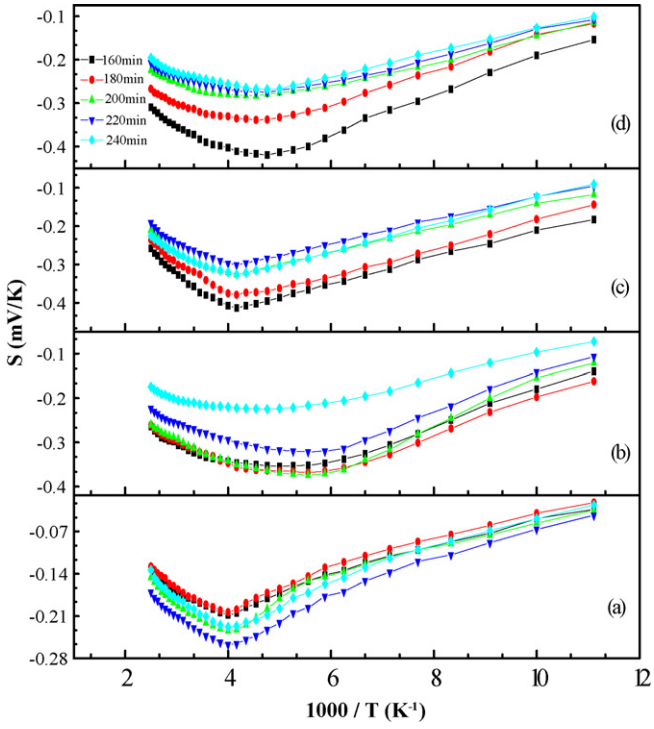

Fig. 5. Temperature dependence of Seebeck coefficient of the alloys $Pb_{1-x}Sm_xSe$: (a) $x = 0.00$; (b) $x = 0.03$; (c) $x = 0.06$ and (d) $x = 0.09$ annealed for different time periods.

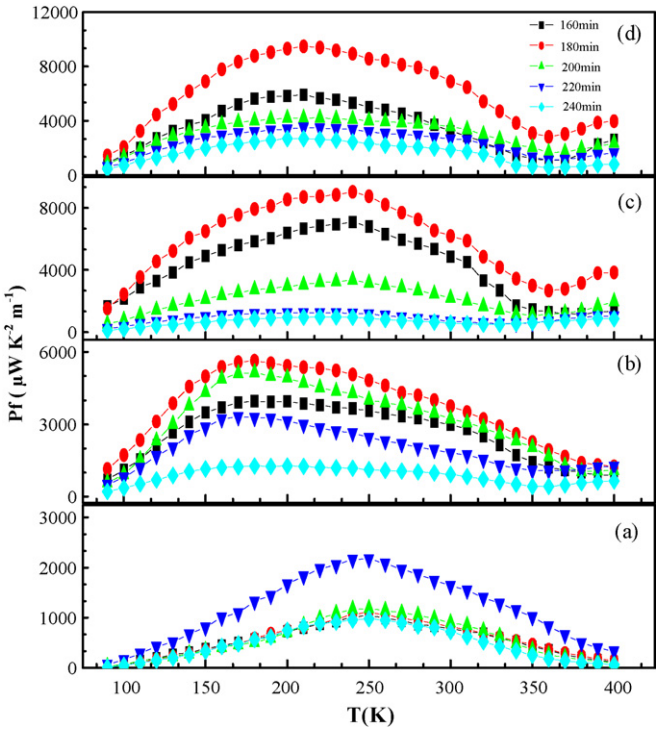

Fig. 7. Temperature dependence of the power factor of the alloys $Pb_{1-x}Sm_xSe$: (a) $x = 0.00$; (b) $x = 0.03$; (c) $x = 0.06$ and (d) $x = 0.09$ annealed for different time periods.

trend is the enhancement of the absolute value of Seebeck coefficient with Sm enriching [29] and the highest value is possessed for $Pb_{0.94}Sm_{0.06}Se$ composition. The reduction of $|S|$ which associates the annealing time prolongation may be attributed to enlarging the grain size which implies a decrease in the number of grain boundaries [18,49].

Fig. 7 shows the temperature dependence of the power factor (Pf) for $Pb_{1-x}Sm_xSe$ compositions. The power factor increased with increasing temperature, showing higher values around 170–250 K, and then decreased. As seen in Fig. 8, the Pf value, at ambient temperature 250 K, increases with Sm content increasing up to $x = 0.06$ for all the concerned time intervals

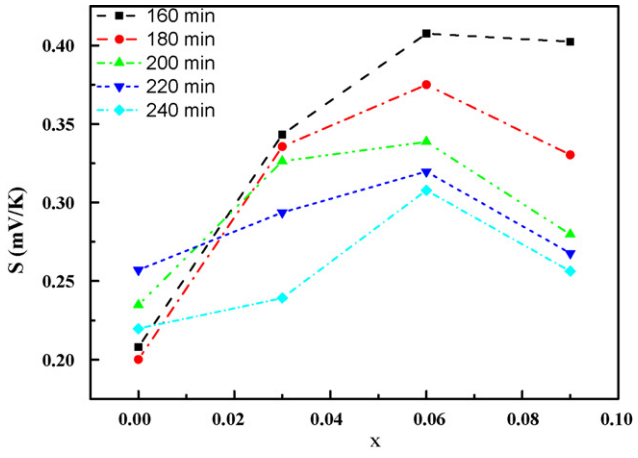

Fig. 6. Modulus value of Seebeck coefficient as a function of Sm content for the investegated compositions after annealing for different time periods.

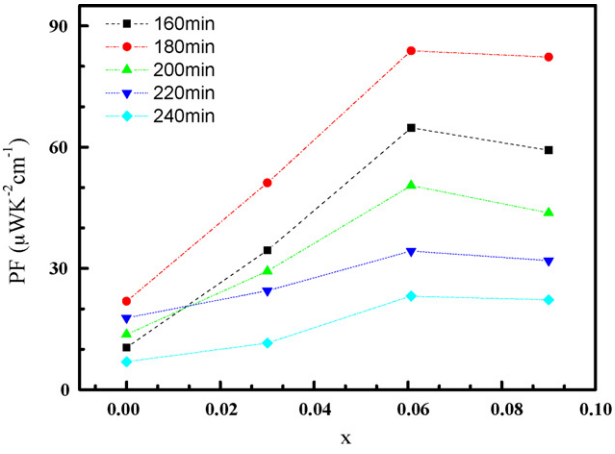

Fig. 8. Power factor at 250 K as a function of Sm content for the investigated samples after annealing for different annealing time periods.

of annealing. Optimizing the doping level and annealing time exhibit highest Pf value for $Pb_{0.94}Sm_{0.06}Se$ sample annealed for 180 min. It is equal to 83.8 $\mu W\,cm^{-1}\,K^{-2}$ which is relatively larger than those published in other works for PbSe compounds.

4. Conclusions

In summary, all the prepared samples are polycrystalline as confirmed by XRD patterns and have NaCl structure. The activation energy values decrease with prolongating the annealing time and increases with increasing Sm content. For all the annealing time intervals, the highest value of Seebeck coeffi-

cient is for 0.06Sm composition. Noteworthy that, adding Sm to PbSe compound enhances much the value of the power factor. The most optimum condition to obtain the highest value of Pf ($83.8\ \mu W\ cm^{-1}\ K^{-2}$) was achieved for $Pb_{0.94}Sm_{0.06}Se$ composition annealed for 180 min. This indicates the role of annealing time and appropriate doping with Sm in changing the carrier concentration, hence their effect on the value of power factor. More detailed investigations of the compounds are now in progress.

References

[1] I.Na. Chao, P.J. McCann, W.L. Yuan, E.A. O'Rear, S. Yuan, Thin Solid Films 323 (1998) 126.
[2] F.J. Meca, M.M. Quintas, F.J.R. Sanchez, Sensors Actuators 84 (2000) 45.
[3] E.Ya. Glushko, V.N. Evteev, Semiconductor 31 (1997) 756.
[4] Z. Dashevsky, S. Shusterman, M.P. Dariel, J. Appl. Phys. 92 (2002) 1425.
[5] R.A. Orozco, M. Sotelo-Lerma, R. Ramirez-Bon, M.A. Quevedo-Lopez, O. Mendoz-Gronzalez, O. Zelaya-Angel, Thin Solid Films 343–344 (1999) 587.
[6] I. Pop, C. Nascu, V. Ionescu, E. Indrea, I. Bratu, Thin Solid Films 307 (1997) 240.
[7] H. Zogg, A. Fach, J. John, J. Masek, P. Muller, C. Paglino, W. Butter, Opt. Eng. 33 (1994) 1440.
[8] S. Chatterjee, U. Pal, Opt. Eng. 32 (1993) 2923.
[9] Q. Li, Y. Ding, M. Shao, J. Wu, G. Yu, Y. Qian, Mater. Res. Bull. 38 (2003) 539.
[10] T. Story, Acta Phys. Polym. A 92 (1997) 663.
[11] G. Nimtz, B. Schlicht, R. Dornhaus, Narrow Gap Semiconductor, Springer, Berlin, 1983.
[12] B.A. Akimov, A.V. Dmitrev, D.R. Khokhlov, L.I. Ryabova, Phys. Status Solidi A 9 (1993) 137.
[13] V.I. Kaoedanov, Y.I. Ravich, Usp. Fiz. Nauk 51 (1985) 145.
[14] T. Story, Act. Phys. Polym. A 94 (1998) 189.
[15] R. Breschi, V. Fano, J. Mater. Sci. 20 (1985) 2990.
[16] K. Nakamura, K. Morikawa, H. Owada, K. Miura, K. Ogawa, I.A. Nishida, in: K. Matsubara (Ed.), Proceedings of the Twelfth International Conference on Thermoelectrics, Inst. Electrical Engineers of Japan, Tokyo, 1994, p. 110.
[17] M. Iizuka, S. Sugihara, J. Jpn. Soc. Powder Metall. 42 (1995) 507 (in Japanese).
[18] H. Unuma, N. Shigetsuka, M. Takahashi, K. Masui, J. Mater. Sci. Lett. 17 (1998) 1055.
[19] S.V. Ovsyannikov, V.V. Shchennikov Jr., N.A. Shaydarova, V.V. Shchennikov, A. Misiuk, D. Yang, I.V. Antonova, S.N. Shamin, Physica B 376–377 (2006) 177.
[20] X. Zhang, X.M. Li, T.L. Chen, L.D. Chen, J. Cryst. Growth 286 (2006) 1.
[21] I.I. Vanckik, D.R. Khokhlov, A.V. Morozov, A.A. Tarekhov, E.I. Slyn'ko, V.I. Slyn'ko, A. de Visser, W.D. Dobrowlski, Phys. Rev. B 61 (2001) 889.
[22] M.M. Ibrahim, E.M.M. Ibrahim, S.A. Saleh, A.M. Abdel Hakeem, J. Alloys Compd. (2006), in press.
[23] T. Story, Z. Wilamowski, E. Grodzicka, B. Witkowska, W. Dobrowlski, Act. Phys. Pol. A 84 (1993) 773.
[24] E. Grodzicka, W. Dobrowolski, T. Story, E. Grodzicka, T. Story, E.I. Slynko, Y.K. Vygranenko, M.M.H. Willekens, H.J.M. Swagten, W.J.M. de Jonge, Act. Phys. Polym. A 90 (1996) 801.
[25] R. Denecke, L. Ley, G. Springholz, G. Bauer, Phys. Rev. B 53 (1996) 4534.
[26] T. Story, M. Gorska, A. Lusakowski, M. Arciszewska, W. Dobrowolski, E. Grodzicka, Z. Gołacki, R.R. Gałazka, Phys. Rev. Lett. 77 (1996) 3447.
[27] X. Grantens, S. Charar, M. Averous, S. Isber, J. Deportes, Z. Golacki, Phys. Rev. B 56 (1997) 8199.
[28] E.P. Skipetrov, N.A. Chernova, L.A. Skipetrova, A.V. Golubev, E.I. Slyn'ko, Semiconductors 35 (2001) 1249.
[29] E.P. Skipetrov, N.A. Chernova, L.A. Skipetrova, E.I. Slyn'ko, Mater. Sci. Eng. B 91–92 (2002) 412.
[30] G. Bauer, H. Pascher, W. Zawadzki, Semiconductors Sci. Technol. 7 (1992) 703.
[31] W.C. Goltsos, A.V. Nurmikko, D.L. Partin, Solid State Commun. 59 (1986) 183.
[32] G. Karczewski, J.K. Furdyna, D.L. Partin, C.N. Thrush, J.P. Heremans, Phys. Rev. B 46 (1992) 13331.
[33] T. Su, P. Zhu, H. Ma, G. Ren, J. Guo, Y. Imai, X. Jia, J. Alloys Compd. 422 (2006) 328.
[34] P.K. Khanna, V.V.V.S. Subbarao, M. Wagh, P. Jadhav, K.R. Patil, Mater. Chem. Phys. 93 (2005) 91.
[35] H. Du, C. Chen, R. Krishnan, T. Krauss, J.M. Harbold, F. Wise, M. Thomas, J. Silcox, Nano Lett. 11 (2002) 1321.
[36] S. Kumar, Z.H. Khan, M.A. Majeed Khan, H. Husain, Curr. Appl. Phys. 5 (2005) 561.
[37] P. Łazarczyk, T. Story, M. Arciszewska, R.R. Gałazka, J. Mag. Mag. Mater. 169 (1997) 151.
[38] A. Svane, V. Kanchana, G. Vaitheeswaran, G. Santi, W.M. Temmerman, Z. Szotek, P. Strange, L. Petitl, Phys. Rev. B 71 (2005) 045119.
[39] K.F. Hsu, S. Loo, F. Guo, W. Chen, J.S. Dyck, C. Uher, T. Hogan, E.K. Polychroniadis, M.J. Kanatzidis, Science 303 (2004) 818.
[40] A. Prinz, G. Brunthaler, Y. Ueta, G. Springholz, G. Bauer, G. Grabeck, T. Dietl, Phys. Rev. B 59 (1999) 12983.
[41] L.A. Kuznetsova, V.L. Kuznetsov, D.M. Rowe, J. Phys. Chem. Solids 61 (2000) 1269.
[42] B. Karmer, A. Mackinnon, Rep. Prog. Phys. 56 (1993) 1469.
[43] S. Espevick, C.H. Wo, R.H. Bube, J. Appl. Phys. 42 (1971) 3523.
[44] F. Briones, D. Gaimayo, C. Ortiz, Thin Solid Films 78 (1981) 385.
[45] A.T. Burkov, A. Heinrich, C. Gladun, W. Pitschke, J. Schumann, Phys. Rev. B 58 (1998) 9644.
[46] Y.M. Xiong1, X.H. Chen, X.G. Luo, C.H. Wang, H.B. Song, C.L. Chen, H.Y. Chang, J. Phys. Condens. Matter 16 (2004) 553.
[47] W. Chen, J.J. Lin, X.X. Zhang, H.K. Shin, J.S. Dyck, C. Uher, Appl. Phys. Lett. 81 (2002) 523.
[48] V.V. Shchennikov, S.V. Ovsyannikov, Solid State Commun. 126 (2003) 373.
[49] J.L. Cui, J. Alloys Compd. 415 (2006) 216.